

A Simplified Approach for Strain-Rate Dependent Hyperelastic Materials with Damage

D.J. Benson¹, S. Kolling², P.A. Du Bois³

¹ University of California, Dept. of Mechanical and Aerospace Engineering, San Diego, USA

² DaimlerChrysler AG, EP/CSB, HPC X411, D-71059 Sindelfingen, Germany

³ Consulting Engineer, Freiligrathstr. 6, 63071 Offenbach, Germany

Abstract

Simulation of rubber-like materials is usually based on hyperelasticity. If strain-rate dependency has to be considered viscous dampers are added to the rheological model. A disadvantage of such a description is time-consuming parameter identification associated with the damping constants. In this paper, a tabulated formulation is presented which allows fast generation of input data based on uniaxial static and dynamic tensile tests at different strain rates. Unloading, i.e. forming of a hysteresis, can also be modeled easily based on a damage formulation. We show the theoretical background and algorithmic setup of our model which has been implemented in the explicit solver LS-DYNA [1]-[3]. Apart from purely numerical examples, the validation of a soft and a hard rubber under loading and subsequent unloading at different strain rates is shown.

*Keywords: Material Modeling Rubber Hyperelasticity Strain-rate Dependency Elastic Damage
parameter identification Explicit Finite Element Method*

1. Introduction

The numerical simulation of structural parts made from rubbers is subject of great interest in such areas as aeronautical and automotive industries. Although highly sophisticated material laws are available in commercial finite element programs, many questions remain open today, especially in the field of crashworthiness analysis. For quasi-static problems, elastomers can be considered as incompressible rubber-like materials. For this class of materials, a large number of models are available in LS-DYNA, e.g. the material laws by Blatz and Ko [4], Mooney [5] and Rivlin [6], Arruda and Boyce [7], Yeoh [8], Ogden [9] and Hill [10]. In short-time dynamics, however, a strong strain rate dependency of elastomers is observed. In crash simulations, the strain rate varies throughout the structure and therefore this aspect of the material response must also be taken into account. To consider rate dependency, the hyperelastic material law has been completed by viscous terms. A disadvantage of such a material description is the large number of parameters which have to be identified for each material. Usually, the parameter identification is quite complex and time consuming. In an industrial environment, only limited time is available to produce simulation results. The most efficient material laws from a user point of view are undoubtedly based on tabulated stress-strain curves obtained directly from physical testing. That way, although some smoothing of the raw test data may be required for reasons of numerical stability, time-consuming fitting operations needed for analytical formulations can be entirely avoided. It should be emphasized, however, that predictable analysis is necessarily based on experimental material testing. In [11], the method has been generalized to foam materials using Hill's functional. Important applications of rubber-like materials and other polymers are given in the overview article [14]. Hysteretic unloading is another aspect of rubber material response that cannot be simulated by hyperelastic models which assume path-independency. In the current paper a damage formulation, see [13], [15], is introduced based on the measured unloading path. The unloading behavior of the rubber is then simulated in a natural way.

2. Hyperelasticity in Principal Stretch Ratios

In a hyperelastic material both stress and deformation energy are path independent functions of the deformation. Together with the requirement of material objectivity, this allows to compute the components of the 2nd PK stress tensor as the derivatives of the energy functional with respect to the Green-Lagrange strain tensor

$$\mathbf{S} = \frac{\partial W}{\partial \mathbf{E}} \text{ where } \mathbf{E} = \frac{1}{2}(\mathbf{F}^T \mathbf{F} - \mathbf{I}) = \frac{1}{2}(\mathbf{C} - \mathbf{I}) = \frac{1}{2}(\mathbf{U}^2 - \mathbf{I}). \quad (1)$$

The right Cauchy-Green tensor \mathbf{C} can only be computed by polar decomposition or by calculating the square root of a matrix using $\mathbf{F} = \mathbf{R}\mathbf{U}$ where $\mathbf{U} = \sqrt{\mathbf{F}^T \mathbf{F}} = \mathbf{U}^T$ and $\mathbf{R}\mathbf{R}^T = \mathbf{I}$. Computing the eigenvectors of \mathbf{C} allows to determine the principal stretch ratios

$$\Phi^T \mathbf{U} \Phi = \begin{pmatrix} \lambda_1 & 0 & 0 \\ 0 & \lambda_2 & 0 \\ 0 & 0 & \lambda_3 \end{pmatrix}, \quad \Phi^T \mathbf{U}^2 \Phi = \begin{pmatrix} \lambda_1^2 & 0 & 0 \\ 0 & \lambda_2^2 & 0 \\ 0 & 0 & \lambda_3^2 \end{pmatrix}, \quad \Phi^T \mathbf{E} \Phi = \frac{1}{2} \begin{pmatrix} \lambda_1^2 - 1 & 0 & 0 \\ 0 & \lambda_2^2 - 1 & 0 \\ 0 & 0 & \lambda_3^2 - 1 \end{pmatrix}.$$

Where in every principal direction $\lambda_i = l_i / l_{0i}$. There is no loss in generality if we express the hyperelastic material law in the principal reference system

$$\Phi^T \mathbf{S} \Phi = \frac{\partial W}{\partial (\Phi^T \mathbf{E} \Phi)} = \begin{pmatrix} s_1 & 0 & 0 \\ 0 & s_2 & 0 \\ 0 & 0 & s_3 \end{pmatrix}, \quad s_i = \frac{\partial W}{\partial \frac{1}{2}(\lambda_i^2 - 1)} = \frac{1}{\lambda_i} \frac{\partial W}{\partial \lambda_i}. \quad (2)$$

In component form we get a very simple expression for the principal second PK components.

For our subsequent derivations we will also need the corresponding expression for the principal true or Cauchy stress values:

$$\Phi^T \mathbf{R}^T \boldsymbol{\sigma} \mathbf{R} \Phi = \frac{2}{J} \Phi^T \mathbf{U} \Phi \frac{\partial W}{\partial \Phi^T \mathbf{U}^2 \Phi} \Phi^T \mathbf{U}^T \Phi \quad (3)$$

All matrices in the right hand side of the last equation are diagonal, consequently we have found the eigenvectors of the Cauchy stress tensor and

$$\sigma_i = \frac{2}{\lambda_1 \lambda_2 \lambda_3} \lambda_i^2 \frac{1}{2\lambda_i} \frac{\partial W}{\partial \lambda_i} = \frac{1}{\lambda_j \lambda_k} \frac{\partial W}{\partial \lambda_i} \quad (4)$$

Note that if true stresses are directly computed we must work in the principal system of the left Cauchy-Green tensor. The most popular formulations for the energy functional in function of the principal stretch ratios are the functionals by Ogden [9] and Hill [10]. The Ogden functional

$$W_o = \sum_{i=1}^3 \sum_{j=1}^m \frac{\mu_j}{\alpha_j} \left(\lambda_i^{*\alpha_j} - 1 \right) + K (J - 1 - \ln J) \quad (5)$$

with $\lambda_i^* = \lambda_i J^{-1/3}$ and $J = VV_0^{-1} = \lambda_1 \lambda_2 \lambda_3$ for nearly incompressible materials and the Hill functional

$$W_h = \sum_{i=1}^3 \sum_{j=1}^m \frac{\mu_j}{\alpha_j} \left(\lambda_i^{\alpha_j} - 1 \right) + \frac{1}{n} \sum_{j=1}^m \frac{\mu_j}{\alpha_j} \left(J^{-n\alpha_j} - 1 \right) \quad (6)$$

for highly compressible materials. The expressions for the principal true stress values can be directly computed by derivation, i.e.

$$\sigma_i = \begin{cases} \frac{1}{\lambda_k \lambda_j} \frac{\partial W_o}{\partial \lambda_i} = \sum_{j=1}^m \frac{\mu_j}{J} \left[\lambda_i^{*\alpha_j} - \sum_{k=1}^3 \frac{\lambda_k^{*\alpha_j}}{3} \right] + K \frac{J-1}{J} & \text{(Ogden)} \\ \frac{1}{\lambda_k \lambda_j} \frac{\partial W_h}{\partial \lambda_i} = \sum_{j=1}^m \frac{\mu_j}{J} \left[\lambda_i^{\alpha_j} - J^{-n\alpha_j} \right] & \text{(Hill)} \end{cases} \quad (7)$$

The small strain modulae are easily determined for the case of the Hill functional as $G = \frac{1}{2} \sum_{j=1}^m \alpha_j \mu_j$ and $K = \left(n + \frac{1}{3} \right) \sum_{j=1}^m \alpha_j \mu_j$.

3. Tabulated Generalization

By defining two functions

$$g_o(\lambda_i) = \sum_{j=1}^m \frac{\mu_j}{\alpha_j} \left(\lambda_i^{*\alpha_j} - 1 \right) \text{ and } g_h(\lambda_i) = \sum_{j=1}^m \frac{\mu_j}{\alpha_j} \left(\lambda_i^{\alpha_j} - 1 \right), \quad (8)$$

the Ogden and Hill functionals can be rewritten as

$$W_o = \sum_{i=1}^3 g_o(\lambda_i) + K(J-1 - \ln J) \text{ and } W_h = \sum_{i=1}^3 g_h(\lambda_i) + \frac{1}{n} g_h(J^{-n}). \quad (9)$$

Similarly we can define two additional functions

$$f_o(\lambda) = \sum_{j=1}^m \mu_j \lambda^{*\alpha_j} \text{ and } f_h(\lambda) = \sum_{j=1}^m \mu_j \lambda^{\alpha_j} \quad (10)$$

and rewrite the expression for the principal true stresses

$$\sigma_i = \frac{1}{J} \left(f_o(\lambda_i) - \frac{1}{3} \sum_{j=1}^3 f_o(\lambda_j) \right) + K \frac{J-1}{J} \text{ and } \sigma_i = \frac{1}{J} (f_h(\lambda_i) - f_h(J^{-n})). \quad (11)$$

The proposed generalization in this work is that we no longer require the functions $g_o(\lambda)$ and $g_h(\lambda)$ to be polynomial. In fact no analytical expression is assumed for them at all. These functions will just be tabulated values of the principal stretch ratios or the relative volume J . The tabulated values will be determined in such a way that available data from uniaxial tension and compression tests is fitted within an arbitrarily small error. Whereas classically the coefficients in the energy functional are determined in order to achieve a best possible overall fit of uniaxial tension, biaxial tension and shear data, it must be recognized that in every day industrial practice, biaxial and shear data are rarely available. A close fit to uniaxial measurements is however very often a practical requirement.

3.1 Uniaxial Test Data

Uniaxial data from tensile and compressive testing is usually recorded as engineering stress versus engineering strain, see Figure 1a.

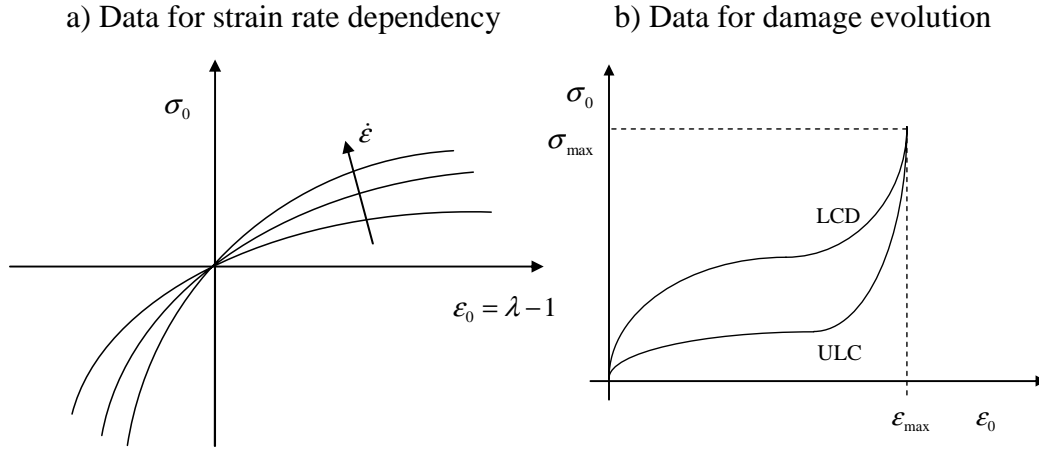


Figure 1: Input data from uniaxial tests

Simple integration gives the deformation energy per unit undeformed volume:

$$W_u(\lambda) = \int_0^{\epsilon_0} \sigma_0 d\epsilon_0 = \int_0^{\lambda} \sigma_0 d\lambda = W_u(\epsilon_0), \tag{12}$$

where $\sigma_0(\epsilon_0) = \sigma_0(\lambda - 1)$ is tabulated in input and $\lambda = \epsilon_0 + 1$. The purpose of the current work is to derive tabulated values for the functions $g_o(\lambda)$, $g_h(\lambda)$ and $f_o(\lambda)$, $f_h(\lambda)$ from the uniaxial engineering stress-strain data that are provided as user input. This conversion between tabulated functions will generate perfect agreement between experimental data and the numerical response under uniaxial loading without any parameter fitting:

3.2 Computation of the Functions $g_o(\lambda)$ and $g_h(\lambda)$

In the case of the Ogden functional we are considering a nearly incompressible material and the uniaxial test conditions can be expressed as follows:

$$g_o(\lambda_i) = \sum_{j=1}^m \frac{\mu_j}{\alpha_j} (\lambda_i^{*\alpha_j} - 1) = W_u(\lambda_i) - 2W_u(\lambda_i^{-1/2}) + 4W_u(\lambda_i^{1/4}) - \dots \tag{13}$$

where $J \approx 1$, $\lambda_j^* = \lambda_k^* = \lambda_i^{*-1/2}$ and $\lambda_j = \lambda_k \approx \lambda_i^{-1/2}$. We will use these terms to compute an expression for the deviatoric part of the deformation energy under uniaxial loading for an Ogden material. The series expression for $g_o(\lambda)$ theoretically continues ad infinitum but since the deformation energy is zero in the undeformed state the practical computation can be terminated once a reasonable number of terms have been evaluated:

$$\text{for } \left| \lambda_i^{(-1/2)^m} - 1 \right| \leq 0.01 : g_o(\lambda_i) = W_u(\lambda_i - 1) + \sum_{m=1}^{\infty} (-2)^m W_u(\lambda_i^{(-1/2)^m} - 1). \tag{14}$$

In the case of the Hill functional the material is compressible and uniaxial conditions are expressed as follows

$$\lambda_j = \lambda_k = \lambda_i^{\frac{-n}{2n+1}}, \quad J = \lambda_i^{\frac{1}{2n+1}}, \quad n = \frac{\nu}{1-2\nu} \quad (15)$$

This time we evaluate the total deformation energy, including the volumetric and deviatoric parts, for the uniaxial case

$$W_u(\lambda_i) = \sum_{j=1}^m \frac{\mu_j}{\alpha_j} (\lambda_i^{\alpha_j} - 1) + \frac{2n+1}{n} \sum_{j=1}^m \frac{\mu_j}{\alpha_j} (\lambda_i^{-\alpha_j n / (2n+1)} - 1)$$

$$W_u(\lambda_i^{-n/(2n+1)}) = \sum_{j=1}^m \frac{\mu_j}{\alpha_j} (\lambda_i^{-\alpha_j n / (2n+1)} - 1) + \frac{2n+1}{n} \sum_{j=1}^m \frac{\mu_j}{\alpha_j} \left(\lambda_i^{-\alpha_j \left(\frac{n}{2n+1}\right)^2} - 1 \right)$$

Again, the evaluation of the series can be terminated once the considered stretch ratio approaches unity

$$\text{for } \left| \lambda_i^{\left(\frac{-n}{2n+1}\right)^m} - 1 \right| \leq 0.01 : g_h(\lambda_i) = W_u(\varepsilon_{0i}) + \sum_{m=1}^{\infty} \left(-\frac{2n+1}{n} \right)^m W_u \left(\lambda_i^{\left(\frac{-n}{2n+1}\right)^m} - 1 \right) \quad (16)$$

where 0.01 is a chosen tolerance. Remark that both formulations coincide if the material is incompressible, i.e. Poisson's ratio $\nu = 0.5 \Leftrightarrow n = \infty$.

3.3 Computation of the Functions $f_o(\lambda)$ and $f_h(\lambda)$

We start by expressing the engineering stress under uniaxial loading for an Ogden material:

$$\sigma_{0i}(\lambda_i - 1) = \frac{\lambda_k \lambda_j}{J} \left(\frac{2}{3} f_o(\lambda_i) - \frac{2}{3} f_o(\lambda_i^{-1/2}) \right) + K \frac{J-1}{J}$$

$$\Leftrightarrow \lambda_i \sigma_{0i}(\lambda_i - 1) = f_o(\lambda_i) - f_o(\lambda_i^{-1/2}) \quad (17)$$

We write expression (17) for consecutive values of the stretch ratio and obtain

$$\lambda_i^{(-1/2)^{m-1}} \sigma_{0i} \left(\lambda_i^{(-1/2)^{m-1}} - 1 \right) = f_o \left(\lambda_i^{(-1/2)^{m-1}} \right) - f_o \left(\lambda_i^{(-1/2)^m} \right). \quad (18)$$

The function $f_o(\lambda)$ is now easily derived by summation:

$$f_o(\lambda_i) = f_o(1) + \lambda_i \sigma_{0i}(\lambda_i - 1) + \lambda_i^{-1/2} \sigma_{0i}(\lambda_i^{-1/2} - 1) + \lambda_i^{1/4} \sigma_{0i}(\lambda_i^{1/4} - 1) + \dots$$

Note that the function $f_o(\lambda)$ is not necessarily zero for a stretch ratio equal to unity. If a

polynomial formulation is chosen as in (10) we have in particular $f_o(1) = \sum_{j=1}^m \mu_j$. With the

current derivation it is not possible to determine the value of $f_o(1)$. However it can be seen that the value of $f_o(\lambda)$ in the stress-free state will not affect the computed stress values. Consequently we can neglect the value of $f_o(\lambda)$ for $\lambda = 1$ and just evaluate

$$f_o(\lambda_i) = \lambda_i \sigma_{0i}(\lambda_i - 1) + \lambda_i^{-1/2} \sigma_{0i}(\lambda_i^{-1/2} - 1) + \lambda_i^{1/4} \sigma_{0i}(\lambda_i^{1/4} - 1) + \dots \quad (19)$$

This series is then truncated as usual

$$\text{for } \left| \lambda_i^{(-1/2)^m} - 1 \right| \leq 0.01 : f_o(\lambda_i) = \sum_{m=0}^{\infty} \lambda_i^{(-1/2)^m} \sigma_{0i} \left(\lambda_i^{(-1/2)^m} - 1 \right). \quad (20)$$

Note that if $f_o(\lambda)$ can be expressed as a polynomial function we have approximated the following expression with the series

$$f_o(\lambda) = \sum_{j=1}^m \mu_j \lambda^{*\alpha_j} - \sum_{j=1}^m \mu_j = \sum_{j=1}^m \mu_j \left(\lambda^{*\alpha_j} - 1 \right). \quad (21)$$

This is the same as equation (10) up to a constant value and will result in the same values for the true stress. The function $f_h(\lambda)$ is obtained in the same way. For the implementation, it is important to realize that the computation of the functions $g_{o,h}(\lambda)$ and $f_{o,h}(\lambda)$ described above need only be done once, e.g. during the initialization of the problem. The procedures described above have been implemented in LS-DYNA as MAT_SIMPLIFIED_RUBBER. User input consists of a uniaxial engineering stress-strain curve covering both the tensile and compressive regions. Additional input required is only the bulk modulus for the Ogden formulation and Poisson’s ratio for the Hill formulation.

3.5 Examples

In a first series of examples, single element tests are performed for loading with prescribed velocities in uniaxial tension, uniaxial compression, simple shear and hydrostatic compression. Corresponding deformed shapes are shown in the Figure 2a. Three different material models have been compared.

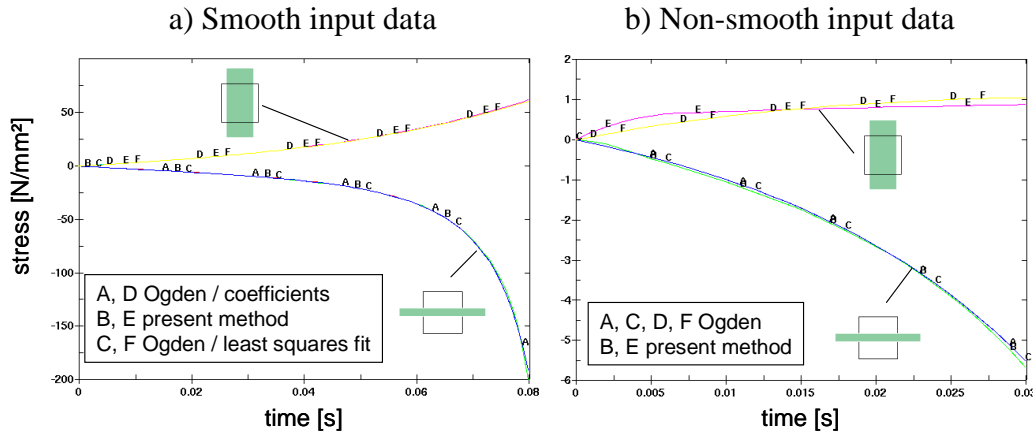


Figure 2: Tensile and compression tests

The first row of elements use a classical Ogden formulation in LS_DYNA (material No. 77) based on input of the coefficients for the energy functional. Based on these coefficients, the uniaxial stress-strain curve was computed by hand and provided as input for the present formulation which has been implemented as MAT_SIMPLIFIED_RUBBER (material No. 181) in LS-DYNA. As a backup-check, the same stress-strain curve was used as input for the Ogden law using a least squares fit of the energy functional. As expected all three models yield exactly the same response in uniaxial tension and compression, see figure 2b. It is, however, more

important to verify that the stress-strain response of the three models is also identical under simple shear and hydrostatic compression loading:

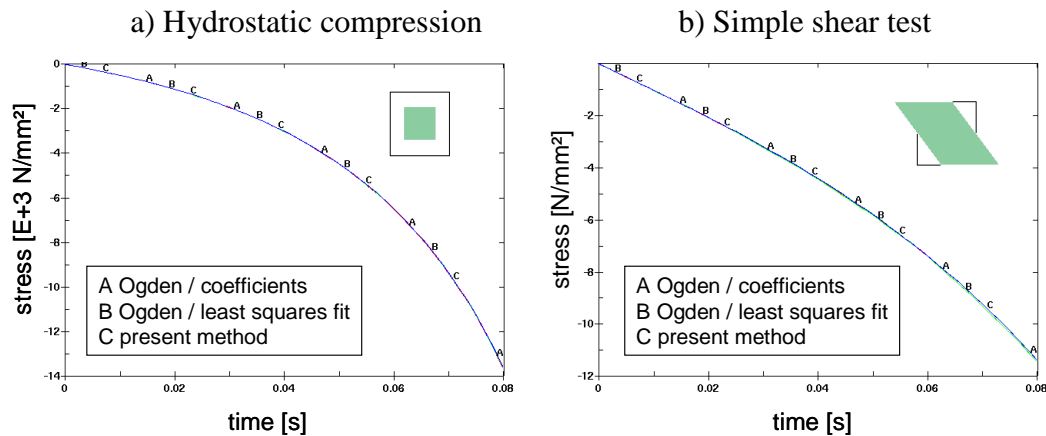


Figure 3: Hydrostatic compression and simple shear test

This shows that although the MAT_SIMPLIFIED_RUBBER requires input concerning the uniaxial response only, the multi-axial behaviour of this material law is fully equivalent to the Ogden model. In a second example, uniaxial tension and uniaxial compression tests were again performed on single element models. This time the present model MAT_SIMPLIFIED_RUBBER and the Ogden law have been used with the same load curve giving the stress-strain response of a hypothetical material. A particular feature of this load curve is that the initial tangent modulae in tension and compression are different. This type of response is actually measured frequently in biological tissues and rubber foams. The problem with such a continuous but non-smooth curve is that the least squares approach in MAT_OGDEN can never produce an exact fit of the test data whereas this poses no problem for the MAT_181. The computed stress-strain curves are shown in figure 2b. Our generalized tabulated approach only requires the stress to be a continuous function of strain. In the Ogden model polynomial functions are used for the energy which always result in differentiable functions for the stress after differentiation. Note, though, that the hyperelastic character of the material would be lost if the energy function would not be differentiable.

Rate Dependency

It is well known that the dynamic response of rubber can be significantly different from the static behaviour. Hysteresis, creep, stress-relaxation and rate effects can all be explained by the visco-elastic nature of this material. A strain rate proportional stress or viscous stress is added to the strain dependent static stress component. Though for many cellular materials such as foams, the physical explanation of the dynamic or rate effects may not be just in the viscosity of the cell wall material. Other effects such as the outflow of air from the cell structure may also have an influence. We have therefore decided to consider rate effects in a purely phenomenological way without implementing any fluid structure interaction for the dynamic stress increase. In the present model, the load curve defining the stress-strain response of the material can simply be replaced by a table containing an arbitrarily high number of load curves. Each load curve defines the stress-strain response in loading at a different strain rate. This approach is much more general than visco-elasticity since any change in shape of the load curves due to the loading velocity is accommodated without any problem. However, obviously certain limitations exist also.

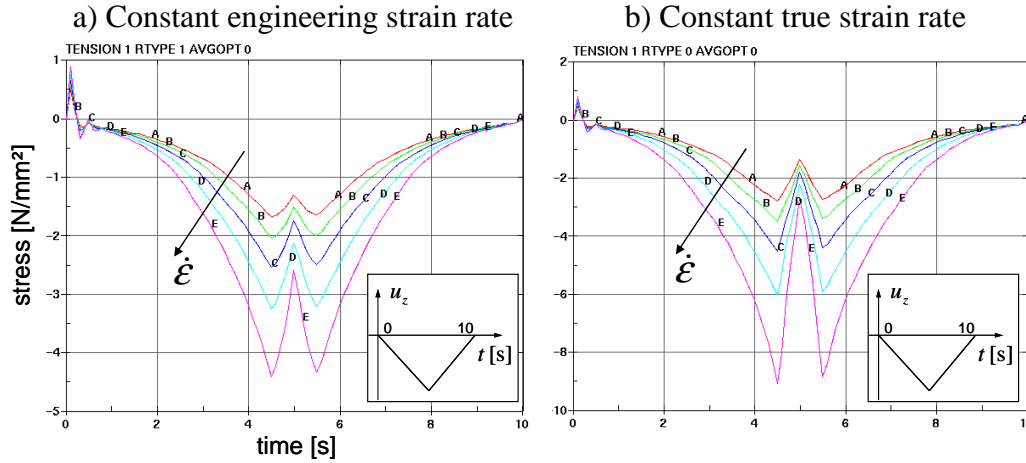


Figure 4: Influence of strain rate definition

To illustrate these limitations we perform a simple uniaxial compression-tension test with unloading on 5 single element structures. The loading is done with a fixed velocity and all 5 elements have different initial heights resulting in different strain rates for each structure. The user defines if the individual load curves in the table were obtained at constant true strain rate (RTYPE=0) or constant engineering strain rate (RTYPE=1). The results of course will differ accordingly. It should be noted that dynamic test results at constant true strain rate are difficult to obtain and engineering strain rate (constant velocity) is the more likely case in daily practice.

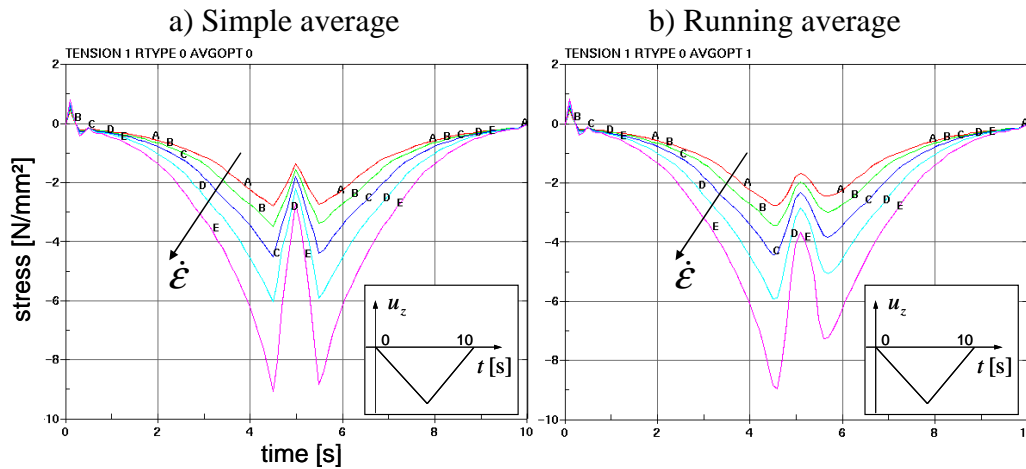


Figure 5: Influence of strain rate averaging

The main limitation of this rate-dependent elastic material model is that the response to a change in loading velocity is instantaneous. As can be seen from the pictures above, when the velocity changes from positive to negative at the point of maximum intrusion, the strain rate actually goes through the zero-point and the stress consequently goes down to the static value. In a real viscous material, relaxation effects would damp such sudden stress changes. Since the velocity will change more gradually in real life load cases, this is not considered to be an important draw-back of the material model. A second limitation results from the necessity to smooth the computed strain rate values over time in explicit solvers. LS-DYNA offers the possibility of a 12 point

simple average (AVGOPT=0) or a 12 point running average (AVGOPT=1). And again this choice will influence the computed stress values, see figure 5.

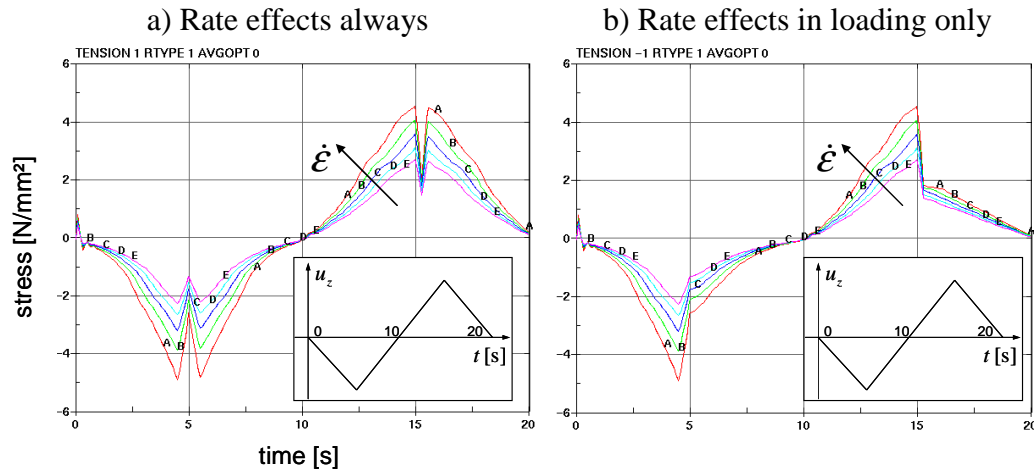


Figure 6: Suppressed rate effects in unloading

The main limitation of the current model however is in the simulation of the unloading phase. To illustrate our implementation, the example above is repeated with two loading/unloading cycles. The unloading response of MAT_SIMPLIFIED_RUBBER is controlled by the user through the input parameter TENSION. In the simplest case (TENSION=1) rate effects are applied in all cases (loading, unloading, tension and compression). This may seem to be the most physical option but it is also numerically the more problematic one since instabilities are sometimes difficult to avoid.

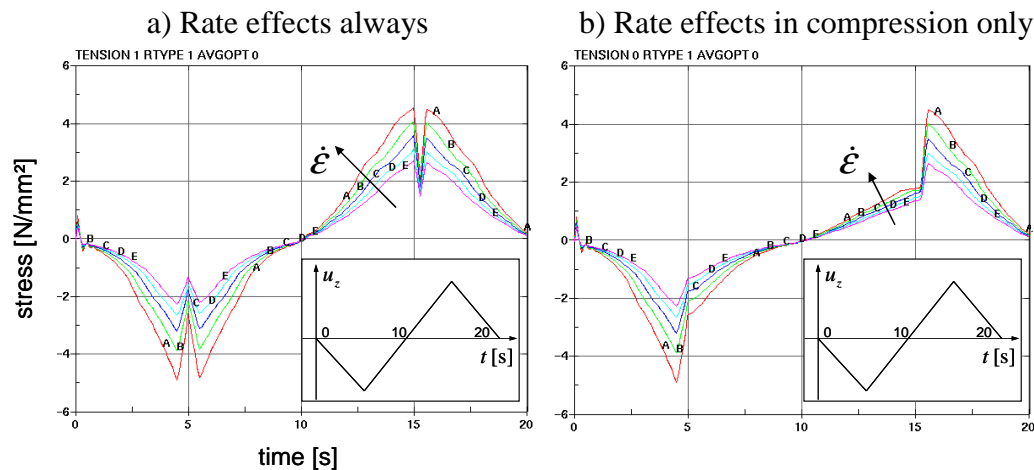


Figure 7: Suppressed rate effects in tension

Therefore, two alternative formulations have been implemented: rate effects in compression only (TENSION=0) and rate effects in loading only (TENSION=-1). The latter option is numerically the more stable one. Loading and unloading in a principal direction are easily defined as $\varepsilon \dot{\varepsilon} < 0 \Rightarrow$ unloading and $\varepsilon \dot{\varepsilon} > 0 \Rightarrow$ loading. All three approaches are illustrated in figures 6 and 7. It should be noted that the option TENSION=0 can easily lead to energy generation under tensile loads since unloading paths can be computed that lay above the loading path. This is, of course, thermodynamically inadmissible.

4. Damage Formulation

To include damage in the material model the energy functional can be multiplied by a damage function. It is customary to apply the damage to the deviatoric part only in the case of an Ogden functional.

$$W_{do} = (1 - d) \sum_{i=1}^3 \sum_{j=1}^m \frac{\mu_j}{\alpha_j} (\lambda_i^{*\alpha_j} - 1) + K (J - 1 - \ln J) \quad (22)$$

$$W_{dh} = (1 - d) \sum_{j=1}^m \left[\sum_{i=1}^3 \frac{\mu_j}{\alpha_j} (\lambda_i^{\alpha_j} - 1) + \frac{1}{n} \frac{\mu_j}{\alpha_j} (J^{-n\alpha_j} - 1) \right]$$

The principal true stresses can no longer be computed directly from the energy functional since due to the damage the material has become path-dependent and a one-to-one relationship between stress and strain no longer exists, i.e. the hyperelastic character of the material is lost:

$$\sigma_i \neq \frac{1}{\lambda_j \lambda_k} \frac{\partial W}{\partial \lambda_i} \quad (23)$$

However by using the second law of thermodynamics an expression for the principal true stresses can still be obtained

$$\sigma_i = (1 - d) \frac{1}{\lambda_j \lambda_k} \frac{\partial W_o}{\partial \lambda_i} + K \frac{J - 1}{J}, \quad \sigma_i = (1 - d) \frac{1}{\lambda_j \lambda_k} \frac{\partial W_h}{\partial \lambda_i} \quad (24)$$

It is thus sufficient to compute the undamaged stress values and multiplied by (1-d).

4.1 Damage Formulation for Unloading

In this case, a loading and unloading engineering stress-strain curve that form a closed loop must be provided by the user, see Figure 1b. The damage parameter d will be a function of the ratio of current deformation energy over maximum deformation energy that was attained during the loading history so far. From these data the damage parameter d can be tabulated as a function of the energy ratio:

$$W_{\max} = V_0 \int_0^{\varepsilon_{\max}} \sigma_{0,lcd} d\varepsilon_0 = \int_0^{\varepsilon_{\max}} \sigma_{0,lcd} d\varepsilon_0, \quad W(\varepsilon_0) = \int_0^{\varepsilon_0} \sigma_{0,lcd} d\varepsilon_0 \quad (25)$$

$$d \left(\frac{W(\varepsilon_0)}{W_{\max}} \right) = 1 - \frac{\sigma_{ulcd}(\varepsilon_0)}{\sigma_{lcd}(\varepsilon_0)} \Rightarrow 0 \leq d \leq 1$$

If two closed loops are provided by the user corresponding to tension and compression, the resulting damage value is taken from the tensile side if $J > 1$ and from the compressive side if $J < 1$.

This formulation was implemented recently in the LS-DYNA package as a material law named “*MAT_SIMPLIFID_RUBBER_WITH_DAMAGE*”. It is available for the Ogden material only.

4.3 Examples

Two rubber materials have been tested experimentally for validation of the numerical model. The experimental setup depends on the load direction. For compression tests, the setup consists of two pressure plates with the cube-like rubber specimen (6x6x6mm) in between. The lower

pressure plate is supported by a load cell. For tensile tests, the specimen is fixed additionally by gluing to the pressure plates, see left hand side of Figure 8.

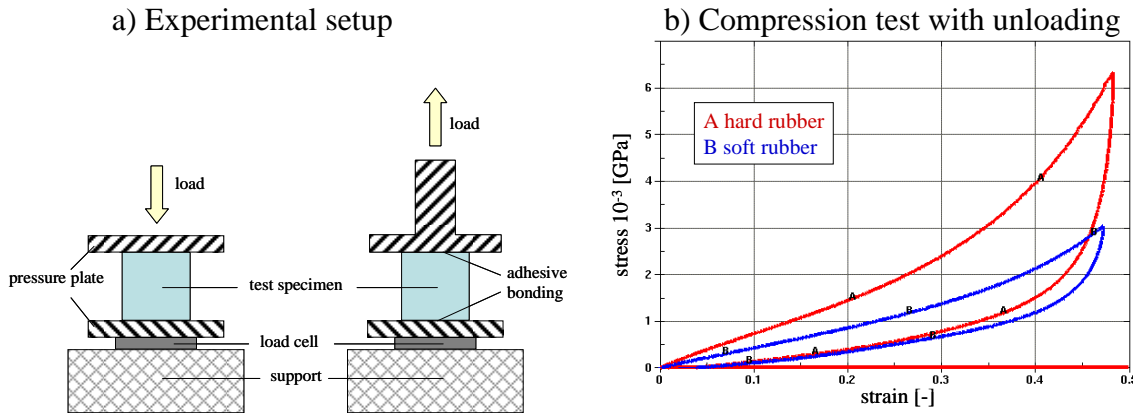


Figure 8: Experimental setup and data of compression test

Compression tests with unloading on rubber cubes were performed for a hard (shore 70) and a weak (shore 55) rubber, see right hand side of Figure 8. Moreover, dynamic tensile tests at different strain rates (0.01/s, 1/s and 100/s) without unloading were also realized for validation.

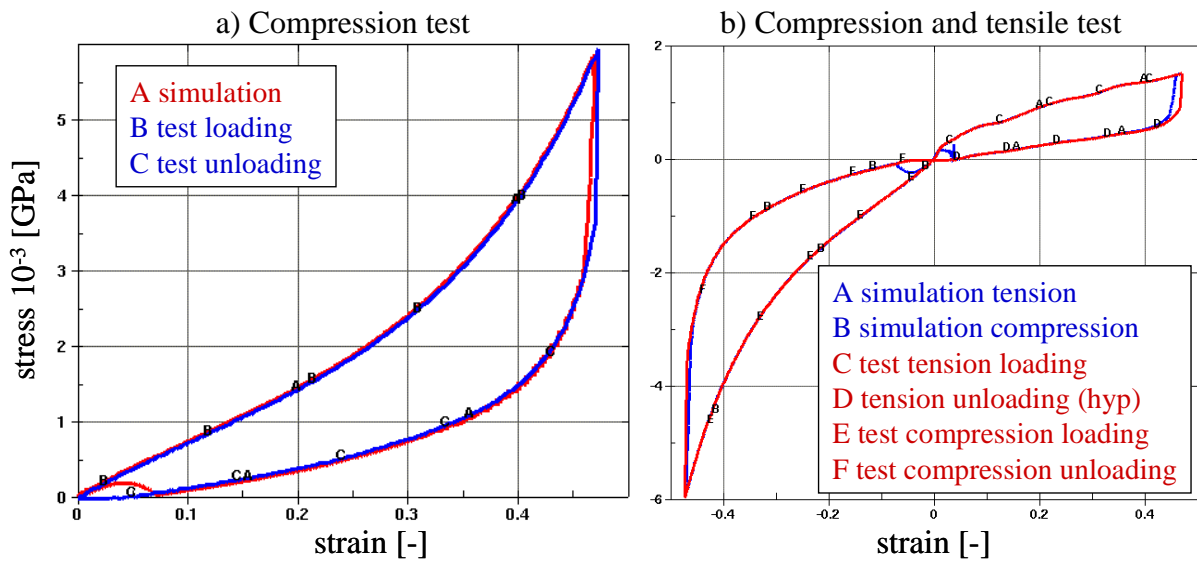


Figure 9: Simulation of loading and unloading (hard rubber)

In Figure 9, the simulation of the compressive test with unloading for the hard rubber is shown.

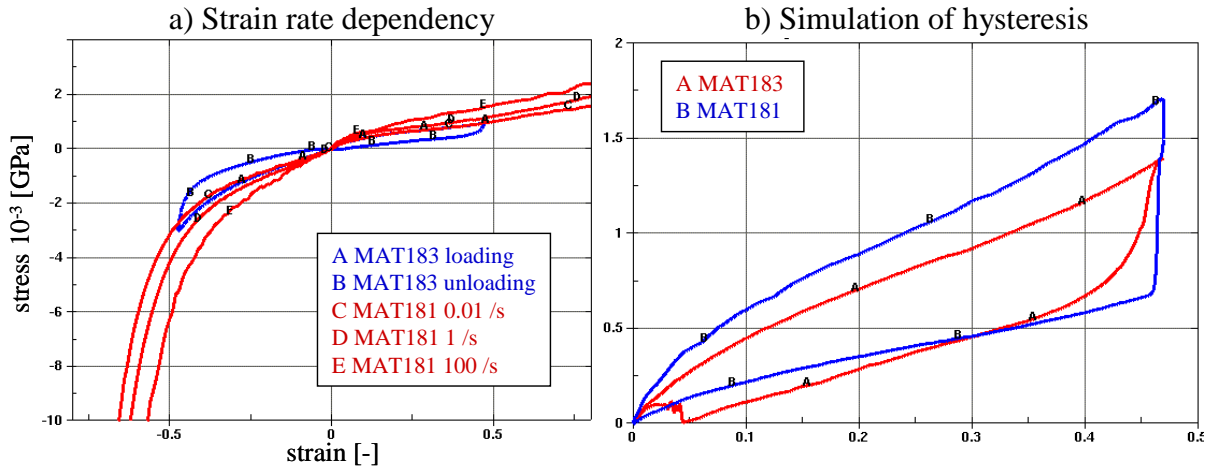


Figure 10: Comparison MAT_183 and MAT_181

Next, we compare the material laws MAT_181 and its extension with damage MAT_183. First some remarks concerning LS-DYNA 9.71 and higher:

- MAT_183 is available also for strain rate dependent materials, i.e. the load curve can be replaced by a table definition referring to the load curves at different strain rates.
- MAT_181 has an extension with a damage model. This is, however, intended for the simulation of failure rather than for the simulation of unloading!

For the simulation of a hysteresis loop, MAT_181 can be used if the unloading is determined by the definition of the strain rate. In Figure 10a), the exact curves simulating the experiment are depicted. In Figure 10b), the strain rate sensitivity is artificially increased to obtain a hysteresis loop in the quasi static case. Note that in this case, the material response for higher strain rates may be not exact anymore.

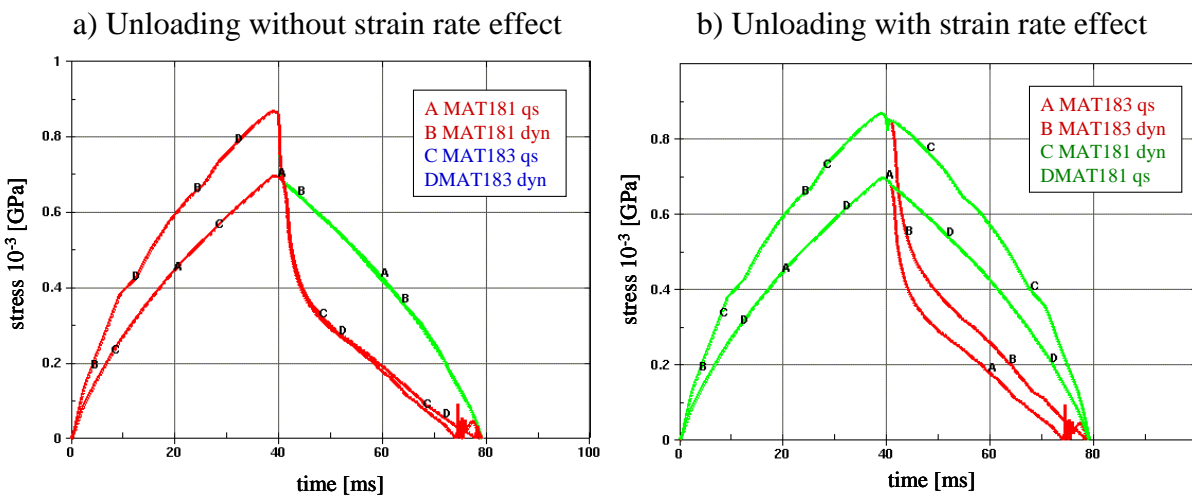


Figure 11: Comparison MAT_183 and MAT_181

In our last validation example, we simulate the strain rate dependency of the soft rubber again in single element tensile tests with unloading. In Figure 11, we compare the material response of MAT181 and MAT183. For each material two tensile loads (with and without rate effects) are simulated resulting in the same maximum deformation. We then perform the analyses twice to illustrate the effect of different settings of the unloading flag TENSION. For TENSION=-1 (Figure 11a), rate effects are considered in the loading phase only. Consequently, the unloading path follows the quasistatic curve in MAT_181 and dynamic and quasistatic unloading paths are identical in MAT_183. For TENSION =1 (Figure 11b) rate effects are considered in loading and unloading phase. Loading and unloading path are then identical for MAT_181 resulting in a potentially unstable material model.

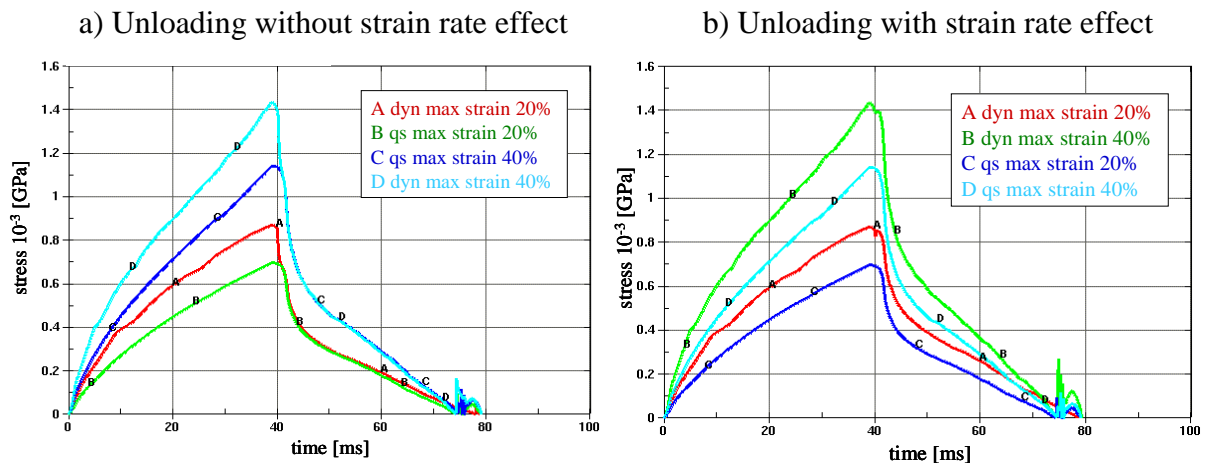


Figure 12: Strain-rate dependency using MAT_183

With MAT_183 the unloading paths show rate dependency and (due to the damage formulation) are always below the loading path. The advantages of MAT_183 upon unloading are clear: rate effects can be considered; damage formulation ensures energy dissipation and hence numerical stability. In Figure 12, tensile tests with and without rate effects are again considered for MAT_183 only. This time different maximum deflections (corresponding to different strain rates upon loading) are applied. It is shown again that for TENSION=-1, quasistatic and dynamic unloading path coincide whereas for TENSION=1, rate effects are clearly present also upon unloading.

5. Summary and Outlook

With the presented material formulation, exact simulation of test data for different strain rates in tension and compression can be achieved without any parameter fitting. Furthermore, stable and realistic unloading behavior with energy dissipation is obtained based on a solid theoretical basis. The implementation has been done for solid and shell elements and is currently limited to the nearly incompressible case (Ogden functional). In the near future the damage formulation will be made available for the general hyperelastic formulation (Hill functional) also. In principle this methodology could be used to fit biaxial data as well as uniaxial data, however convergence seems to become an issue in this case. Future development will concentrate on failure via damage and generalization to anisotropic materials.

References

- [1] LS-DYNA User Manual and Theoretical Manual, Livermore Software Technology Corporation
- [2] Du Bois, P.A. (2004): Crashworthiness Engineering Course Notes, Livermore Software Technology Corporation
- [3] Du Bois, P.A.; Kolling, S.; Fassnacht, W. (2002): Material modeling with LS-DYNA for crashworthiness analysis. LS-DYNA Forum, Bad Mergentheim, Germany, V2:1-56
- [4] Blatz, P.J.; Ko, W.L. (1962): Application of Finite Elastic Theory to the Deformation of Rubbery Materials. *Transaction of the Society of Rheologie*, 6, 223-251
- [5] Mooney, M. (1940): A Theorie of Elastic Deformations. *Journal of Applied Physics* 11, 582-592
- [6] Rivlin, R.S. (1948): Large Elastic Deformations of Isotropic Materials. *Fundamental Concepts, Philosophical Transactions of the Royal Society of London, Series A* 240, 459-490
- [7] Arruda, E.M.; Boyce, M.C. (1993): A three-dimensional constitutive model for the large stretch behavior of rubber elastic materials. *J. Mech. Phys. Solids*, Vol. 41, 389-412.
- [8] Yeoh, O.H. (1990): Characterisation of Elastic Properties of Carbon-Black-Filled Rubber Vulcanisates. *Rubber Chemistry and Technology* 63, 792-805
- [9] Ogden, R.W. (1982): Elastic Deformations of Rubberlike Solids. *Mechanics of Solids*, In: Hopkins, H.G, Sewell, M.J. (eds.); *The Rodney Hill 60th Anniversary Volume*, Pergamon Press, Oxford
- [10] Hill, R. (1978): Aspects of invariance in solid mechanics, *Adv. Appl. Mech.* 18: 1-75
- [11] Du Bois, P.A. (2003): A simplified approach for the simulation of rubber-like materials under dynamic loading. 4th European LS-DYNA Users Conference, pp. D-I-31/46
- [12] Feng, W.W. (2003): On constitutive equations for elastomers and foams. 4th European LS-DYNA Users Conference, pp. D-II-15/28
- [13] Kolling, S.; Benson, D.J.; Du Bois, P.A. (2005): A simplified rubber model with damage. 4th LS-DYNA Forum, Bamberg, 2005, Conference Proceedings, ISBN 3-9809901-1-7, pp. B-II-01/10
- [14] Du Bois, P.A.; Kolling, S.; Koesters, M.; Frank (2006), T: Material behaviour of polymers under impact loading. *International Journal of Impact Engineering* 32: 725-740
- [15] Miehe, C. (1995): Discontinuous and Continuous Damage Evolution in Ogden-Type Large Strain Elastic Materials, *European Journal of Mechanics, A/Solids* 14, 697-720